Catalysis Today 158 (2010) 178–185

Contents lists available at ScienceDirect

Catalysis Today

journal homepage: www.elsevier.com/locate/cattod

Correlation between theoretical and experimental investigations of the ammonia adsorption process on the (1 1 0)-$VSbO_4$ surface

Elizabeth Rojas[a], Mònica Calatayud[b,*], M. Olga Guerrero-Pérez[c], Miguel A. Bañares[a,*]

[a] Catalytic Spectroscopy Laboratory, Instituto de Catálisis y Petroleoquímica, CSIC, Marie Curie 2, E-28049 Madrid, Spain
[b] UPMC CNRS Univ Paris 06, UMR 7616, Laboratoire de Chimie Théorique, F-75005 Paris, France
[c] Departamento de Ingeniería Química, Universidad de Málaga, E-29071 Málaga, Spain

ARTICLE INFO

Keywords:
DFT
Adsorption
NH_3
$VSbO_4$
Vanadium
Antimony
Rutile

ABSTRACT

Ammoxidation reactions involve the activation of ammonia and its subsequent oxidation in order to obtain the desired nitrile. In this paper the role of NH_3 interaction with the activity and selectivity of $VSbO_4$ catalysts is investigated. Experimental data reveal that the catalyst ability to adsorb ammonia is related with its catalytic behaviour. Moreover, ammonia adsorption drives the formation of the active $VSbO_4$ rutile phase for metal oxide contents close to the monolayer. Periodic DFT calculations indicate that ammonia strongly adsorbs on Brønsted sites, while Lewis acid sites lead to a favourable dissociation to NH_2 and NH. It is demonstrated that the adsorption of NH_3 and NH_x preferentially involves isolated vanadium sites. The isolated vanadium sites in the vicinity of antimony sites seem to provide a unique local environment for the initial steps of the ammoxidation reaction.

1. Introduction and objectives

Metals and metal oxides are active catalysts for the oxidation and/or ammoxidation of hydrocarbons. The catalytic behaviour of these two groups of substances is determined by their surface electronic properties, which, in the conditions of the oxidation process, can be explained by the existence of a semiconductor coating on the metal surface [1,2]. For the clarification of the main regularities of the process, it is necessary to break the reaction scheme into elementary steps. One of the main steps in this process is the adsorption of the reactants (O_2, NH_3 and hydrocarbons). Ammonia acts as reactant in two main industrial reactions: (i) the ammoxidation of hydrocarbons (alkenes, alkanes, alkylaromatics) to the corresponding organic nitriles and (ii) the reduction of NO by NH_3, in the presence of O_2, being the first step for the production of nitric acid. Thus, a study concerning NH_3 adsorption on the surface of catalysts is a fundamental work with applied industrial relevance.

V-Sb oxide based catalysts are a preferred formulation for the ammoxidation of propane to acrylonitrile [3–9], as well as for other reactions [10]. Experimental studies have been made about the adsorption of NH_3 on V-Sb oxide surface and about the nature of the chemisorbed ammonia species [5–8]. Despite the large experimental effort applied to the system, the nature of the NH_3-derived adsorbed species has not been definitely addressed. Ammonia is bonded to the surface mainly in two different modes. First, physisorption can be considered as a precursor state of the subsequent chemisorbed molecule [11]. Next, the molecule interacts strongly with the surface leading to chemisorbed species. These chemisorbed species are either ammonium ions coming from ammonia protonated by a proton from a surface hydroxyl group, probing surface Brønsted acid sites; or the lone pair electron of the nitrogen atom binds to the metal cation, which acts as a Lewis acid site. Thus, one of the most important points in order to clarify the ammoxidation mechanisms is to characterize the adsorption states of both ammonia and the corresponding hydrocarbon, which are directly related to the reaction pathway, giving an insight into the initial steps of the catalytic reaction.

The nature of the chemisorbed ammonia species determines the intrinsic surface reactivity and selectivity of V-Sb-O catalysts in the synthesis of acrylonitrile. Centi et al. [11] showed that the oxidation of propane involves a complex reaction network and suggested that the rates of the various competitive pathways depend on the surface acid properties of the catalyst, which would be considerably modified by adsorption of a base such as NH_3. The most commonly used method involves spectroscopic investigation of adsorbed probe molecules. The chemisorption of ammonia seems to be crucial in the surface reactivity of V-Sb-oxide. TPD and DRIFT spectroscopic studies reveal that short lived NH_x species (most probably $NH_{3,ads}$ or NH_4^+) are active in the formation of acrylonitrile from propane [12]. These species are also involved in the formation of the non-selective side-product N_2, which would proceed via NO and N_2O. As far as we know, no theoretical study directly addresses ammonia adsorption on any surface of $VSbO_4$; there are, however, some studies on the

* Corresponding author. Tel.: +33 1 44 27 26 82; fax: +33 1 44 27 41 17.
E-mail address: calatayu@lct.jussieu.fr (M. Calatayud).

0920-5861/$ – see front matter © 2010 Elsevier B.V. All rights reserved.
doi:10.1016/j.cattod.2010.03.071

adsorption of ammonia on V_2O_5 (0 1 0) [13] and on the adsorption of another molecule (toluene) on $VSbO_4$. Yin et al. [13] reported density functional calculations on a periodic (0 1 0) surface model, showing that adsorption takes place on both Brønsted and Lewis acid sites, but the adsorption on the Brønsted sites is energetically more favourable; due to that, the ammonium species forms when ammonia molecules adsorb at the hydroxyl group formed in the vanadyl oxygen. Calatayud et al. [14] found that NH_3 dissociation to NH_2 + H is favoured on vanadia based on cluster model B3LYP calculations. Irigoyen et al. [15] have studied the adsorption of toluene on a (1 1 0) surface cluster model of $VSbO_4$, the H-abstraction from toluene to produce a stable benzyl species represents the first step in the oxidation reaction and phenyl-V interactions weakens V–O bonds while C–H bonds remain unchanged. In the present work we present a periodic model for the (1 1 0) surface of $VSbO_4$ used to determine both the surface adsorption sites and the ammonia adsorption modes and strength for the first time.

$VSbO_4$ is a key phase for propane ammoxidation. The synthesis and structure of $VSbO_4$ have been reported in detail. Birchall and Sleigth [16] reported a synthesis method for $VSbO_4$, which exhibited a tetragonal rutile-type structure. In this structure, the Sb and V ions are present as Sb^{5+} and V^{3+}. Hansen et al. [17] reported a rutile-type $VSbO_4$ structure with a Sb:V = 1 ratio, with different metal–oxygen probable combinations. They concluded that this oxide presents a cation deficient rutile phase leading to the formation of coordinative unsaturated oxygen species. In the same study a bond valence analysis suggested that $OSb_2\square$, $OSbV\square$, and $OV_2\square$ are the most favourable arrangements (the square $\square$ denotes cation vacancies). To the best of our knowledge, the adsorption of molecules on V-Sb oxides has only been addressed for toluene [27], but no theoretical study of this system has been reported for ammonia.

In this work a combined experimental and theoretical study is presented in order to determine the role of the ammonia adsorption in the catalytic behaviour during the ammoxidation of propane to acrylonitrile. Experimentally activity and selectivity of this catalytic reaction are studied and correlated with the presence of a $VSbO_4$ phase as well as with its acidity, measured as the consumption of NH_3. Both the molecular and the dissociative adsorption of ammonia as NH or NH_2 have been explored in detail by means of periodic DFT calculations. The role of Lewis and Brønsted surface acid sites is thus discussed and compared with the experimental results.

2. Experimental section

2.1. Preparation of catalysts

The Sb-V catalysts were prepared dissolving the required amount of antimony acetate (Aldrich) in tartaric acid (Sigma) 0.3 M. This solution was kept under stirring until all antimony dissolves. Then, NH_4VO_3 (Sigma) and the γ-Al_2O_3 (Sasol, Puralox SCCa-5/200) support were added. The solution was dried in a rotatory evaporator at 80 °C and 0.3 atm. The resulting solid was dried at 115 °C for 24 h and then calcined at 400 °C for 4 h in air. The catalysts were prepared so that a total coverage of V + Sb would correspond to 50% and 100% of the dispersion limit, understood as the maximum surface loading of VO_x units at which they remain dispersed, with no crystalline V_2O_5. Such value was determined by Raman spectroscopy to be near 9 VO_x units per nm^2 for alumina and niobia supports, in accordance to previous reports [18]. The catalyst nomenclature is based on total coverage of alumina support and on the stoichiometry. Thus they are named as *x*Sb*y*V*z* where "*x*" indicates the number of monolayers of V + Sb atoms on alumina support, "*y*" and "*z*" indicate the atomic *y*/*z* stochiometry of Sb/V atoms. Thus, 0.5SbV2 indicates a total coverage of half monolayer of V + Sb, with a vanadium molar content twice that of antimony.

2.2. Characterization

Nitrogen adsorption isotherms (−196 °C) were recorded with an automatic Micromeritics ASAP-2000 apparatus. Prior to the adsorption experiments, samples were outgassed at 140 °C for 2 h. BET areas were computed from the adsorption isotherms (0.05 < P/Po < 0.27), taking a value of 0.164 nm^2 for the cross section of the adsorbed N_2 molecule at −196 °C. ICP analyses were made on a PerkinElmer – 3300 DV-Disgreggation. The samples were disaggregated with a microwave oven using HNO_3, HF and HCl. X-ray diffraction patterns were recorded on a Siemens Krystalloflex D-500 diffractometer using Cu Kα radiation (λ = 0.15418 nm) and a graphite monochromator. Working conditions were 40 kV, 30 mA, and scanning rate of 2°/min for Bragg's angles (2 h) from 5 to 70°. In some cases, the peaks of Al from the sample holder are present. The ammonia chemisorption experiments were performed on an ASAP-2000 apparatus. The catalysts (200 mg) were pre-treated at 250 °C for 0.5 h and then cooled to 100 °C under He flow. This procedure has been proved to efficiently remove water from the catalyst [19]. The pre-treated samples were exposed to 5% NH_3/He, with subsequent flushing with helium at 100 °C for 1 h to remove the physisorbed ammonia. These acidity values were determined from the difference between ammonia adsorption and desorption isotherms.

2.3. Activity measurements

Activity measurements were performed using a conventional microreactor with on-line gas chromatograph, equipped with a flame ionization and thermal-conductivity detector and with a Porapak Q column and molecular sieve. Correctness of the analytical determinations was checked for each test by verification that the carbon balance (based on the propane converted) was within the cumulative mean error of the determinations (±10%). Yields and selectivities in products were determined based on the moles of propane feed and products, considering the carbon balance in each molecule. To prevent participation of homogeneous reaction, the reactor was designed to minimize gas-phase activation upstream and downstream the catalyst bed and was made of quartz. Upstream the catalyst bed, the reactor consisted of a 9 mm o.d. (7 mm i.d.) quartz tube; downstream the catalyst bed, the reactor consisted of a capillary 6 mm o.d. (2 mm i.d.) quartz tube. The axial temperature profile was monitored by a thermocouple sliding inside the closed 6 mm o.d. quartz tube inserted into the catalytic bed. The catalysts were pre-treated in flowing air at 450 °C for 30 min. The reaction mixture feed was $C_3H_8/O_2/NH_3/He$ = 9.8/25/8.6/56.6. The tests were made using 0.20 g of sample with a particle size in the range 0.250–0.125 mm; the total flow rate was 20 ml/min corresponding to a gas-space velocity (GHSV) of 3000 h^{-1}; experimental-conditions outer of diffusional limitations.

2.4. DFT calculation method

2.4.1. Computational details

The calculations are performed with the Vienna Ab initio Simulation Package VASP [20,21] based on the density functional theory (DFT). The Perdew-Wang 91 (PW91) functional form is employed. The core electrons are replaced by PAW (projector-augmented-wave approach) generated pseudopotentials, and the valence electrons are described by plane waves with a cutoff energy of 400 eV. The valence electrons are the following: O: $2s^2 2p^4$ Sb: $5s^2 5p^3$ V: $4s^2 3d^3$ N: $2s^2 2p^3$ H: $1s^1$. The Brillouin zone is sampled

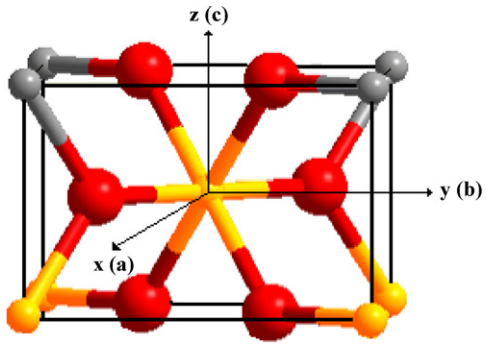

Fig. 1. Primitive unit cell for compounds with rutile AB_2 structure, (A) yellow and grey, and (B) red. (For interpretation of the references to color in this figure legend, the reader is referred to the web version of the article.).

by a Monkhorst-Pack grid of $3 \times 2 \times 1$ k-points (dimensions of the surface cell: $6.610 \times 9.373 \times 26\,\text{Å}^3$). A vacuum space of at least 10 Å prevents the interaction between successive slabs. This approach can provide useful information about the electronic structure of transition metal oxides as well as about the interactions between the adsorbed molecules and the catalyst surface.

2.4.2. Model

The primitive unit cell for AB_2 compounds with rutile structure is shown in Fig. 1. In this structure, each metal atom A coordinates octahedrically with six nearest oxygen atoms B. Each unit cell contains two AB_2 molecules, or a total of six atoms. The (1 1 0)-$VSbO_4$ surface has been modelled using a trirutile tetragonal super cell (see Fig. 2), which contains the most probably metal–oxygen combinations as reported by Hansen et al [17]. The optimized lattice parameters for $a = b = 4.674$ Å and $c' = 9.373$ Å ($c' = 3c$, $c = 3.1243$ Å) are in excellent agreement with the corresponding experimental ones ($a = 4.636$ Å, $c' = 9.114$ Å). The slab used is four MO_2 layers thick of which the two uppermost MO_2 layers have been relaxed, the bottom are kept fixed to the bulk positions. The surface slab supercell contains six cations (three six-fold, three five-fold) exposed on the surface.

The rutile structure is formed by infinite chains of metal–oxygen octahedra with shared edges and corners. Each metal atom bounds to six oxygen atoms (O) while each oxygen bounds to three metal atoms (M). The metal–metal distances in the resulting structure are always relatively long and there are no effective O..O or *M..M* interactions. Additionally, open channels parallel to z axis are formed in the crystal. The plane (1 1 0) used in our calculations was chosen because it appears to be one of the most stable crystal faces and results from breaking the smallest number of M–O bonds. This surface exhibits an outmost layer of oxygen atoms bridging six-fold metal cations in the most probable combinations reported by

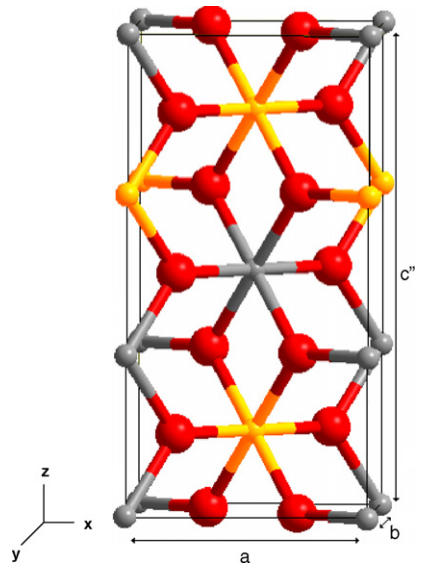

Fig. 2. Tetragonal trirutile-like superstructure of $VSbO_4$, Sb: yellow, V: grey and O: red. (For interpretation of the references to color in this figure legend, the reader is referred to the web version of the article.).

Hansen et al. [17]. The model has been built following the principle of site isolation, a concept proposed for selective catalytic oxidation catalysts [22]. Thus, in the hypothetical slab modelled in this work V sites and Sb ions alternate in two different arrangements: S^A where two Sb-cations are separated by one V cation, and S^B where two neighbouring V-cations are separated by one Sb ion. The different active sites explored in these structures are O, Sb, and V ions as indicated in the Fig. 3. Slab S^A is found to be 0.79 eV more stable than S^B. For the sake of completeness we report the results obtained for the two models.

Full optimization of all the constituent atoms of the adsorbate/substrate system was performed with the conjugate gradient algorithm. The adsorption energy (E_{ads}) has been calculated according to the expression:

$$E_{ads} = E_{(adsorbate/substrate)} - E_{adsorbate} - E_{substrate}$$

where $E_{(adsorbate/substrate)}$, $E_{adsorbate}$, and $E_{substrate}$ are the total energies of the adsorbate/substrate system, isolated adsorbate, and substrate, respectively. A negative E_{ads} value corresponds to a stable adsorbate/substrate system.

3. Experimental study

Fig. 4 shows the XRD patterns of the alumina-supported Sb-V-O catalysts. All the patterns exhibit the peaks of alumina near 46 and

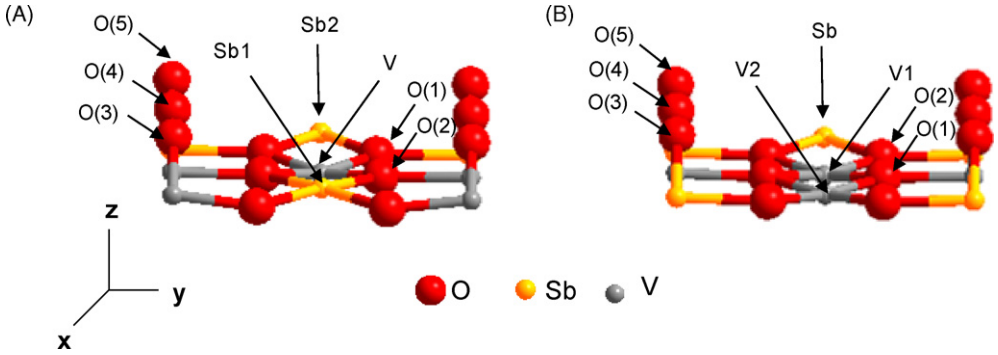

Fig. 3. Positions of the atoms in the (A) S^A and (B) S^B slabs (side view).

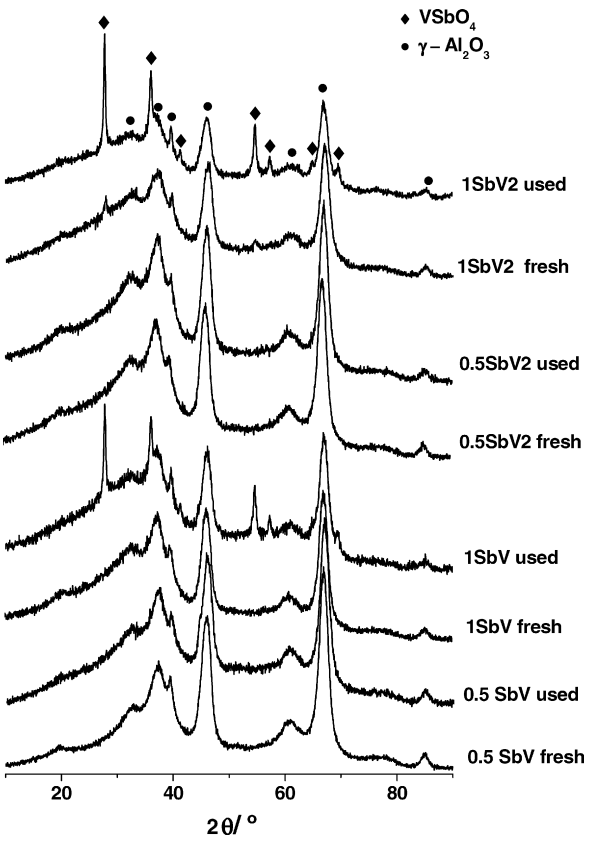

Fig. 4. XRD patterns of the alumina-supported Sb-V-O catalysts fresh and used.

67° (JCPDS file 37-1462). Fresh 1SbV2 shows small peaks that correspond to $SbVO_4$ (JCPDS 16-0600). After reaction, the pattern of $VSbO_4$ becomes also evident for used 1SbV and 1SbV2, indicating that propane ammoxidation favours the formation of $VSbO_4$. Thus, vanadium and antimony react under ammoxidation conditions to form a rutile-like vanadium-antimonate phase ($VSbO_4$) that is the active site, or at least one of the active sites, for acrylonitrile formation [12,17,23,24]. The diffractograms confirm that the formation of the rutile $VSbO_4$ structure is favoured for vanadium and antimony contents close to the monolayer.

Table 1 shows composition, BET area values and activity for propane ammoxidation. Catalysts with low coverage (0.5SbV and 0.5SbV2) present low conversion yield values to acrylonitrile and low ammonia adsorption values. XRD patterns (Fig. 4) indicate that the rutile $VSbO_4$ structure is not detected in these catalysts. On the other hand, ammonia adsorption increases for the catalysts with higher coverage (1SbV and 1SbV2), which afford significantly higher activity and yield values for propane ammoxidation (Table 1). For these catalysts, the formation of the rutile structure during propane ammoxidation is evident by XRD (Fig. 4), especially for the catalysts with higher Sb/V content.

Experimental results show a close link between the presence of the rutile $SbVO_4$ phases, ammonia adsorption and acrylonitrile yield. DFT calculations should provide a rationale on this relationship.

4. Theoretical study: DFT calculation method

4.1. Ammonia adsorption on Lewis acid sites

As a first step, we consider the ammonia molecular adsorption on the Lewis acid sites. (1 1 0)-$VSbO_4$ surface exposes "naked" vanadium and antimony atoms, undercoordinated five-fold sites

Table 1
Composition, BET area, acidity, propane conversion and yield to acrylonitrile at 500 °C. Reaction conditions: total flow 20 ml/min, feed composition (vol%); $C_3H_6/O_2/NH_3$ (9.8:25:8.6), 200 mg of catalysts.

Catalysts	Sb/V ratio	Sb + V "monolayer"	Composition (ICP) (wt%)		BET area ($m^2\ g^{-1}$)	Acidity (μmol NH_3/m^2)	Propane conversion (%)	Acrylonitrile yield (%)
			Sb	V				
0.5SbV	1	0.5	5.1	1.8	181	1.2111	26.3	11.1
1SbV	1	1	8.3	3.0	162	2.1370	68.2	55.2
0.5SbV2	0.5	0.5	3.6	2.3	190	1.2984	36.1	20.8
1SbV2	0.5	1	6.5	4.1	163	2.6073	70.4	56.7

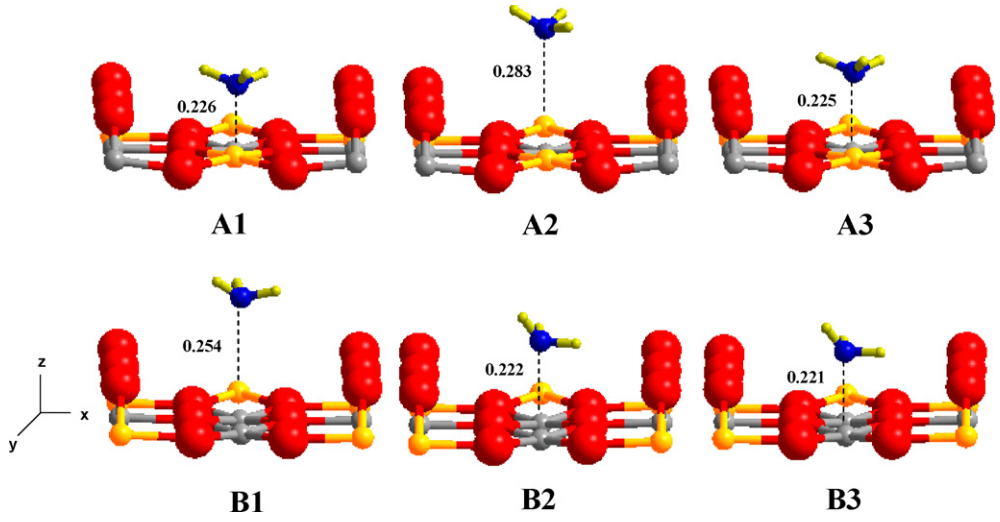

Fig. 5. Fully optimized geometries of ammonia molecule adsorption on the Lewis acid sites present in the (1 1 0)-$VSbO_4$ surface of S^A and S^B slabs. Distances in nm.

Table 2
Adsorption energies with respect to NH_3 adsorption on the Lewis acid sites of (1 1 0)-$VSbO_4$ surface of S^A and S^B slab.

Structure	Sites	Distance C–N[a] (nm)	E_{ads} (kcal/mol)
A1	Sb1	0.226	−24.07
A2	Sb2	0.283	−26.19
A3	V	0.225	−32.84
B1	Sb	0.254	−11.98
B2	V1	0.222	−20.53
B3	V2	0.221	−21.68

[a] C is cation (e.g. V or Sb).

Table 3
Selected parameters on NH_3 adsorption on the Brønsted acid sites of bridging oxygen row on the (1 1 0)-$VSbO_4$ surface of S^A slab and S^B slab.

Structure	Sites		Distance (nm) N–H	Distance (nm) N–O	E_{ads} (kcal/mol)
	NH_3	OH			
AB1	V–O(5)–Sb	V	0.217	0.297	−62.09
AB2	Sb–O(4)–V	V	0.222	0.299	−49.52
AB3	V–O(3)–V	V	0.195	0.277	−56.65
BB1	Sb–O(5)–Sb	V1	0.245	0.302	−41.75
BB2	Sb–O(4)–V	V1	0.243	0.306	−57.00
BB3	V–O(3)–Sb	V1	0.262	0.297	−48.82

which are Lewis acid sites. The adsorption energy and geometry of ammonia on S^A and S^B slabs were calculated at three different sites for each slab: Sb1, Sb2, V and Sb, V1, V2, respectively (Fig. 5). Adsorption of NH_3 on the Lewis acid sites depends on the interaction of its frontier orbitals with the vanadium or antimony atoms. The exposed cations are electron-deficient and can receive electrons from nitrogen lone pairs orbitals of NH_3 through interaction of symmetry-related cation and NH_3 orbitals [25,26].

Table 2 shows the calculated adsorption energy for the two model slabs. The interaction over the A3 structure (V-atom) of S^A slab is the most favourable and the system reaches an adsorption energy value of −32.84 kcal/mol at a C–N distance of 0.225 nm (see Table 2). For the S^B slab the interaction over the B3 structure (V2-atom) is found to be the most favourable reaching an adsorption energy value of −21.68 kcal/mol at a C–N distance of 0.221 nm. Irigoyen et al. [27] showed that the perpendicular interaction toluene with the (1 1 0)-$VSbO_4$ surface on top of a vanadium site is the most favourable, reaching a total energy value of −41 kcal/mol with an optimum distance of 0.211 nm.

We conclude that ammonia binds preferentially to vanadium sites with an exothermic heat of adsorption. The interaction is of electrostatic acid–base character. The preferred site for ammonia adsorption is found to be isolated undercoordinated vanadium surrounded by two antimony sites. However, by infrared spectroscopy chemisorbed NH_3 on Lewis acid sites is found to inhibit the activation of propane, different from that chemisorbed on Brønsted sites [11]. Owing to the difference in the nature of interaction, the adsorption on the Lewis acid sites can be expected to be much weaker than that on the Brønsted acid sites where stronger interaction takes place.

4.2. Ammonia adsorption on Brønsted acid sites

It is generally believed that hydroxyl species present in metal oxide surfaces are formed mainly by the dissociation of water. A model for the Brønsted acid sites has been constructed by formal adsorption of water as OH^- (put on top of the Lewis sites) and H^+ (put on top of the bridging oxygen row). The adsorption energy and geometry of ammonia on (1 1 0)-$VSbO_4$ surface were calculated for three different sites in the S^A and S^B: V–O(3)–V, Sb–O(4)–V and V–O(5)–V in S^A slab, and Sb–O(5)–Sb, Sb–O(4)–V and V–O(3)–Sb, for S^B slab (see Fig. 6). Ammonia molecule strongly adsorbs on these three Brønsted acid sites in the bridging oxygen row at the (1 1 0)-$VSbO_4$ surface (see Fig. 7).

As shown in Table 3, all three adsorption structures in the S^A slab (AB1, AB2 and AB3), are energetically very stable and the adsorption ability decreases in the order corresponding to the hydroxyl groups: O(5)H > O(3)H > O(4)H. This order indicates that the adsorption of ammonia on the V–O(5)–Sb sites is the most favourable with an exothermic interaction of −62.09 kcal/mol.

Fig. 8 shows ammonia adsorption on Brønsted acid sites in the S^B slab. The ammonia adsorption in the BB2 structure (Sb–O(4)–V site) is energetically very stable with total energy of −57.00 kcal/mol (see Table 3). The adsorption ability decreases in the order corresponding to the hydroxyl groups: O(4)H > O(3)H > O(5)H, underlining the preference of ammonia molecule to adsorb at sites in S^B slab that possess vanadium atoms (Table 3).

According to these results, the interaction of ammonia with Brønsted acid sites is stronger than the corresponding Lewis sites in agreement with previous experimental results. Moreover, the preferred site for adsorption is found to be a two-fold hydroxyl site bridging both V and Sb sites. This might be an indication of a unique

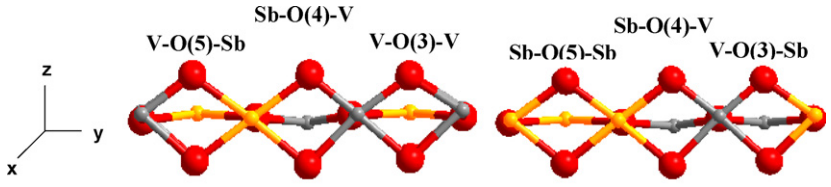

Fig. 6. Brønsted acid sites labelling in S^A and S^B slab (side view). See the text for the description of the models.

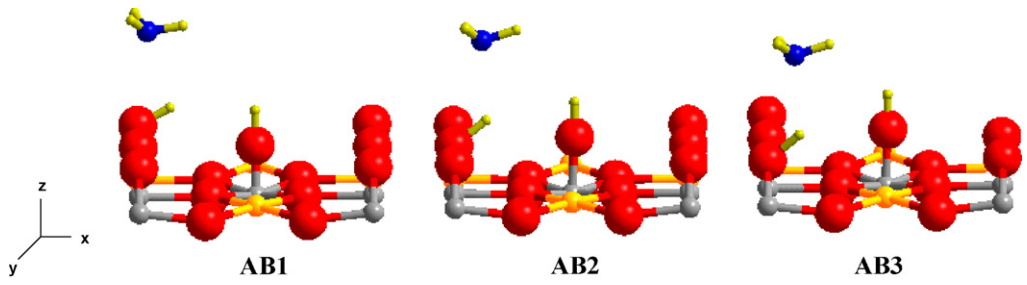

Fig. 7. Geometries of ammonia adsorption at the Brønsted acid sites on the bridging oxygen row on the (1 1 0)-$VSbO_4$ surface of S^A slab.

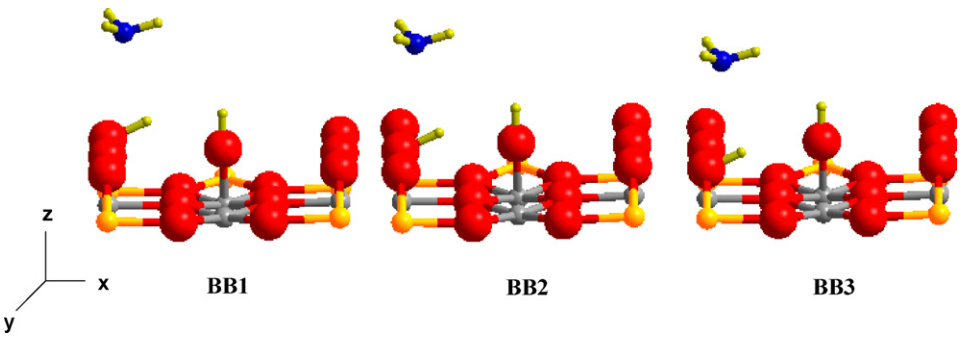

Fig. 8. Geometries of ammonia adsorption at the Brønsted acid sites on the bridging oxygen row on the (1 1 0)-$VSbO_4$ surface of S^B slab.

chemical environment driving the initial steps of the catalytic reaction. However, the strong interaction energy for ammonia adsorption might render such sites inaccessible to hydrocarbons.

4.3. Ammonia activation in (1 1 0)-$VSbO_4$ surface

In order to establish the energetics of the ammonia activation the dissociation to $NH_2 + H$ and $NH + 2H$ has been studied on the Lewis sites. The NH_x species is put on top of the Lewis sites and the H atoms on the bridging oxygen row. Table 4 shows the adsorption

Table 4
Selected parameters the ammonia dissociation to NH_2 and NH on the Lewis acid sites of the (1 1 0)-$VSbO_4$ surface in the S^A slab.

Structure	Sites	Distance C–N[a] (nm)	E_{ads} (kcal/mol)
A4 $NH_2 + H$	Sb1	0.202	−18.93
A5 $NH_2 + H$	Sb2	0.210	−8.37
A6 $NH_2 + H$	V	0.187	−19.32
A7 $NH + 2H$	Sb1	0.195	16.98
A8 $NH + 2H$	Sb2	0.193	29.78
A9 $NH + 2H$	V	0.233	−4.45

[a] C is cation (e.g. V or Sb).

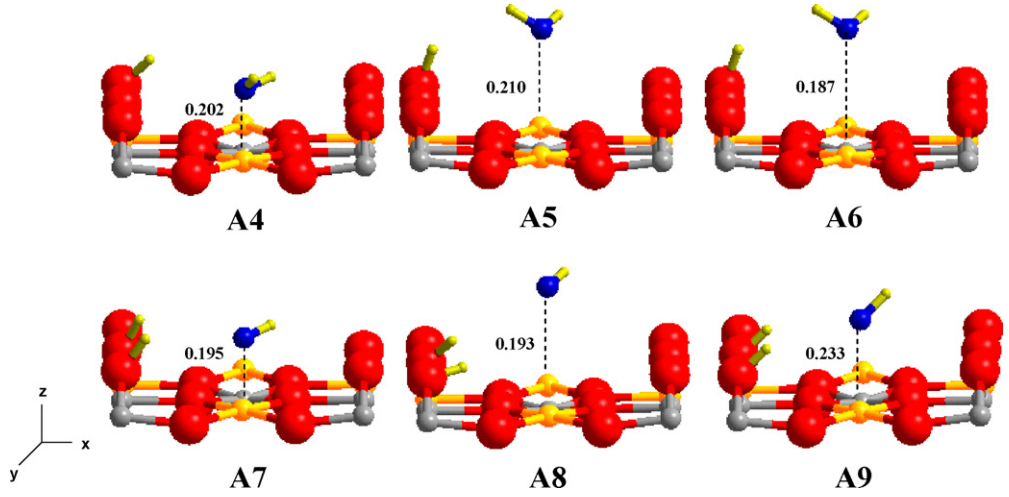

Fig. 9. Fully optimized geometries of NH_2 and NH adsorption on the Lewis acid sites present in the (1 1 0)-$VSbO_4$ surface of S^A slab.

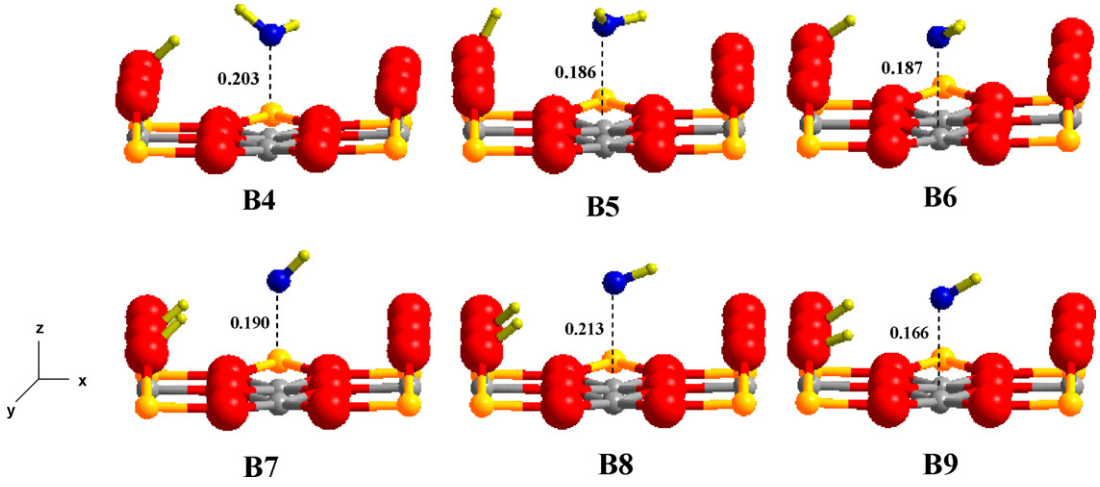

Fig. 10. Fully optimized geometries of NH_2 and NH adsorption on the Lewis acid sites present in the (1 1 0)-$VSbO_4$ surface of S^B slab. Distances in nm.

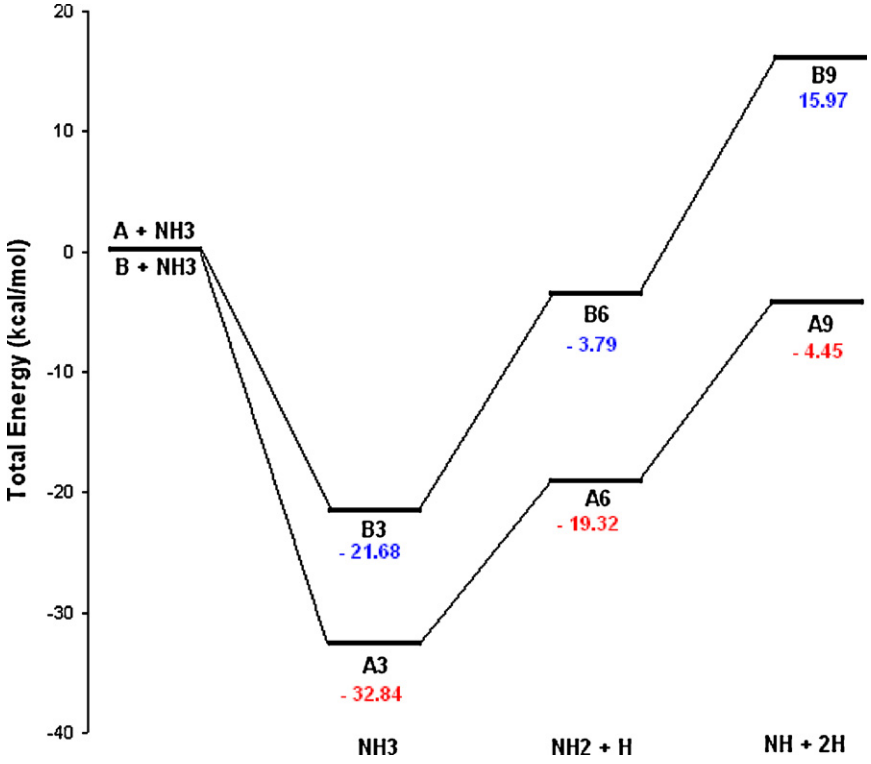

Fig. 11. Potential energy surface for activation of NH_3 on V-sites in the S^A and S^B slab.

energy calculated for the ammonia dissociation to NH_2 and NH at the S^A slab. Fig. 9 shows fully optimized geometries of NH_2 and NH adsorption on the Lewis acid sites present on (1 1 0)-$VSbO_4$ surface at the S^A slab. For NH_2, V-site in the S^A slab is more favourable than Sb-sites (−19.32 kcal/mol at a C-N distance of 0.187 nm). On the S^B slab (Fig. 10), NH_2 adsorbs preferentially on V1 and V2 sites, although more weakly (−6.85 kcal/mol for V1, Table 5). The different stabilities of NH_2 on both S^A and S^B slab deserve particular attention. The difference in the adsorption energy between both surfaces is quite significant. So, in the S^A the adsorbed NH_3 molecule is expected to dissociate to produce NH_2 and H. The adsorption energy is the sum of three contributions: distortion energy of the adsorbed molecule, distortion energy of the surface, and interaction energy of adsorbate-surface. In general, the metal atoms on the adsorption site move upward with a concomitant increase of the C–N bond distances.

It is worth to note that in the case of the S^A slab the dissociation to NH_2 + H and NH + 2H are energetically favourable processes leading to exothermic adsorption energies. The decomposition of NH_3 at the S^A slab to produce NH_2 and NH involve an increase in energy of 13.52 and 14.87 kcal/mol, respectively (see Fig. 11) with respect to the molecular adsorption at the Lewis sites. However, the latest situation is still exothermic (−4.45 kcal/mol, A9) and thus feasible.

Table 5
Selected parameters on the ammonia dissociation to NH_2 and NH on the Lewis acid sites of the (1 1 0)-$VSbO_4$ surface in the S^B slab.

Structure	Sites	Distance C–N[a] (nm)	E_{ads} (kcal/mol)
B4 NH_2 + H	Sb	0.203	4.41
B5 NH_2 + H	V1	0.186	−6.85
B6 NH_2 + H	V2	0.187	−3.79
B7 NH + 2H	Sb	0.190	42.85
B8 NH + 2H	V1	0.213	16.07
B9 NH + 2H	V2	0.166	15.97

[a]C is cation (e.g. V or Sb).

This is consistent with the observed temperature effect, which promotes further dissociation to produce NH_2 and NH. At the S^B slab, the increase in energy for the decomposition of NH_3 into NH_2 and NH is 17.89 and 19.76 kcal/mol, respectively, but in this case the final product NH + 2H is endothermic (15.97 kcal/mol, B9). Thus, the dissociative adsorption of NH_3 to NH_2 and NH, at the S^A slab is supported by our calculations since all the intermediate steps are energetically favourable. Although these considerations are based on thermodynamics, kinetic barriers for the S^A slab are not expected to be high enough to block the decomposition pathway given the thermodynamic stability of the intermediates. We conclude that the presence of isolated undercoordinated vanadium sites neighboring two antimony sites (S^A slab) is able to promote ammonia decomposition.

5. Conclusions

The role of ammonia adsorption on the ammoxidation of propane has been studied from experiments and theoretical DFT calculations. NH_3 experimental adsorption data show that samples with metal (V, Sb) contents close to the monolayer (i) lead to the formation of a $VSbO_4$ phase, the ammoxidation reaction driving its formation (ii) are more favourable for ammonia adsorption and (iii) lead to the highest conversion and selectivity towards acrylonitrile. The calculations show that molecular ammonia adsorption on Brønsted sites is more favourable than on Lewis acid sites. For the Lewis sites, vanadium five-fold sites are preferred for ammonia molecular adsorption, while for the Brønsted sites V–O(5)H–Sb sites are preferred. It has been shown that for isolated vanadium Lewis sites the dissociative adsorption of NH_3 to NH_2 and NH is thermodynamically favourable. The presence of isolated vanadium Lewis sites seems to play a key role in the process. We conclude that neighbouring vanadium-antimony sites constitute a unique local environment that might be responsible for the properties of the $VSbO_4$ catalyst.

Acknowledgments

COST action D36, WG No. D36/0006/06 and the Spanish Ministry of Science and Innovation (grant no. CTQ2008/02461/PPQ) are acknowledged for the financial support. E.R. thanks CONACYT (México) for her pre-doctoral fellowship and COST D36 for the financial support (STSM) during her stay. Authors thank Olaf Torno (SASOL, Germany) for providing the alumina support and R. López-Medina for his help with catalytic tests. This work was performed using HPC resources from GENCI- CINES/IDRIS (Grant 2009-x2009082131, 2010- x2010082131) and the CCRE-DSI of Université P. M. Curie.

References

[1] S.Z. Roginskii, Collect.: Problems Kinet. Catal. 185 (1949) 4.
[2] S.Z. Roginskii, Chem. Sci. Ind. 3 (1956) 138.
[3] M.O. Guerrero-Pérez, J.L.G. Fierro, M.A. Vicente, M.A. Bañares, J. Catal. 206 (2002) 339.
[4] M.O. Guerrero-Peréz, M.V. Martinez-Huerta, J.L.G. Fierro, M.A. Bañares, Appl. Catal. A 298 (2006) 1.
[5] G. Centi, F. Marchi, S. Perathoner, Appl. Catal. A 149 (1997) 225.
[6] G. Centi, S. Perathoner, F. Trifirò, Appl. Catal. A 157 (1997) 143.
[7] G. Centi, S. Perathoner, J. Chem. Soc. Faraday Trans. 93 (1997) 1147.
[8] G. Centi, S. Perathoner, Catal. Rev. -Sci. Eng. 40 (1998) 175.
[9] M.O. Guerrero-Pérez, J.L.G. Fierro, M.A. Bañares, Top. Catal. 41 (1–4) (2006) 43.
[10] M.O. Guerrero-Pérez, J. Janas, T. Machej, J. Haber, A.E. Lewandowska, J.L.G. Fierro, M.A. Bañares, Appl. Catal. B 71 (2007) 85.
[11] G. Centi, F. Marchi, S. Perathoner, J. Chem. Soc., Faraday Trans. 92 (1996) 5151.
[12] H.W. Zanthoff, S.A. Buchholz, O.Y. Ovsitser, Catal. Today 32 (1996) 291.
[13] X. Yin, H. Hao, I. Gunji, A. Endou, S.S.C. Ammal, M. Kubo, A. Miyamoto, J. Phys. Chem. B 103 (1999) 4701.
[14] M. Calatayud, B. Mguig, C. Minot, Surf. Sci. Rep. 55 (2004) 169.
[15] B. Irigoyen, A. Juan, S. Larrondo, N. Amadeo, Surf. Sci. 523 (2003) 252.
[16] T. Birchall, A.W. Sleigth, Inorg. Chem. 15 (4) (1976) 868.
[17] S. Hansen, K. Stahl, R. Nilsson, A. Andersson, J. Solid State Chem. 102 (1993) 340.
[18] I.E. Wachs, L.E. Brian, J.M. Jehng, L. Burcham, X. Gao, Catal. Today 57 (2000) 323.
[19] M.A. Bañares, G. Mestl, Adv. Catal. 52 (2009) 43.
[20] G. Kresse, J. Hafner, Phys. Rev. B 48 (1993) 13115.
[21] G. Kresse, D. Joubert, Phys. Rev. B 59 (1999) 1758.
[22] J.L. Callahan, R.K. Grasselli, AIChE J. 9 (1963) 755.
[23] R.K. Grasselli, Catal. Today 49 (1999) 141.
[24] M.O. Guerrero-Pérez, M.A. Bañares, Chem. Commun. 12 (2002) 1292.
[25] M. Calatayud, A. Markovits, M. Menetrey, B. Mguig, C. Minot, Catal. Today 85 (2003) 125.
[26] M. Calatayud, A. Markovits, C. Minot, Catal. Today 89 (2004) 269.
[27] B. Irigoyen, A. Juan, S. Larrondo, N. Amadeo, J. Catal. 201 (2001) 169.